

**DETECTABILITY OF CRYSTALLINE FERRIC AND FERROUS MINERALS ON MARS:** Donald E. Sabol Jr. (Department of Geological Sciences, University of Washington, Mail Stop AJ-20, Seattle WA 98195), James F. Bell III (NASA/Ames Research Center, Mail Stop 245-3, Moffett Field CA 94035), and John B. Adams (Department of Geological Sciences, University of Washington, Mail Stop AJ-20, Seattle WA 98195)

**Introduction:** Telescopic and spacecraft spectroscopic and geochemical data have been used to constrain the surface mineralogy of Mars and to yield clues about past and present Mars surface weathering/alteration scenarios [1,2]. Based primarily on their visible to near-IR reflectance properties, several terrestrial iron-bearing minerals have been either identified on Mars or proposed as Mars spectral analogs. Among these are crystalline hematite, pyroxenes, as well as poorly crystalline materials like nonophase hematite and palagonite [e.g., 3-6]. Other iron-bearing minerals include (but not limited to) nontronite, magnetite, jarosite, and goethite, have been proposed as Mars surface constituents based on Viking Lander measurements or geochemical modeling [e.g., 7-9]. If present on Mars, these materials likely appear as spectral mixtures at the coarse spatial resolution of remotely sensed data. The detectability of any of these components must be evaluated relative to the other (background) components with which they occur. The primary goal of this study is to determine how much of any given mineral would have to be present for it to be detectable in remotely-sensed data. Here, the detectability of iron-bearing minerals ("target spectra") was evaluated using detection threshold analysis (DTA), an analytical technique based on spectral mixture analysis [10].

**Methods:** DTA is used to predict target detectability (at a given confidence level) under given conditions of target-background spectral contrast and system noise. Two general cases are considered in DTA: 1) Continuum Analysis - the target is treated as a spectral endmember where the "detection threshold" is the smallest fractional abundance of the target that can be measured above system noise, and 2) Residual Analysis - the target, which is not included as an endmember, is detected as deviations of the observed mixed spectrum (including the target) from spectral mixtures of "background" endmembers.

Two sets of background spectra were used: 1) nanophase hematite and magnetite ("pure" phases of iron bearing minerals), and 2) palagonite and lunar basalt (natural materials composed of mineral composites). Spectra of nine target minerals were examined: hematite, goethite, enstatite, hypersthene, diopside, pigeonite, epidote, jarosite, and nontronite. Because the spectral signatures due to iron were primarily of interest, we used high resolution spectra (183 bands) between 0.402  $\mu\text{m}$  and 1.392  $\mu\text{m}$ . Signal-to-noise ratios (SNR) of both 20/1 and 80/1 as well as a confidence level of 90% were used for determining detection thresholds. Because these materials could be expected to occur as both macroscopic and intimate mixtures on Mars, both linear and non-linear mixing (single-scattering-albedo) models were used.

**Results:** Overall, continuum analysis shows that very little of each of these target minerals is needed to be detected within our modeled background, even when the data are noisy. At a SNR of 20/1 the thresholds ranged from 2% to 11%, while at an 80/1 SNR the thresholds were reduced to between 1% and 6.5% (Figure 1). Detection thresholds in residual analysis, which vary by wavelength, ranged from being undetectable to as low as 8% (Figure 2). For most of the minerals examined, residual detectability was highest between 0.4  $\mu\text{m}$  and 0.6  $\mu\text{m}$ . Minerals that have a weaker  $\text{Fe}^{3+}$  crystal field absorption at 0.4  $\mu\text{m}$  were more detectable in this wavelength region than those with stronger absorptions because they had higher spectral contrast with the background, which also had strong absorptions at the lower wavelengths. Generally, the minerals that have weaker  $\text{Fe}^{3+}$  crystal-field bands were more detectable when they were modeled as spectral endmembers than when they were detected in the band residuals.

**Conclusions:** This study indicates that under ideal conditions (i.e., hyperspectral, high-resolution; high solar illumination; no calibration errors) relatively low abundances of crystalline iron-bearing minerals can be detected in spectral mixtures with known background materials. Future refinement of this work will include: 1) accounting for the spectral variability of each mineral (including phase angle and particle size effects), 2) more complex combinations

of spectral components, 3) selection of bands that optimize detection of these minerals, and 4) extension to image analysis of Mars using telescopic and spacecraft data.

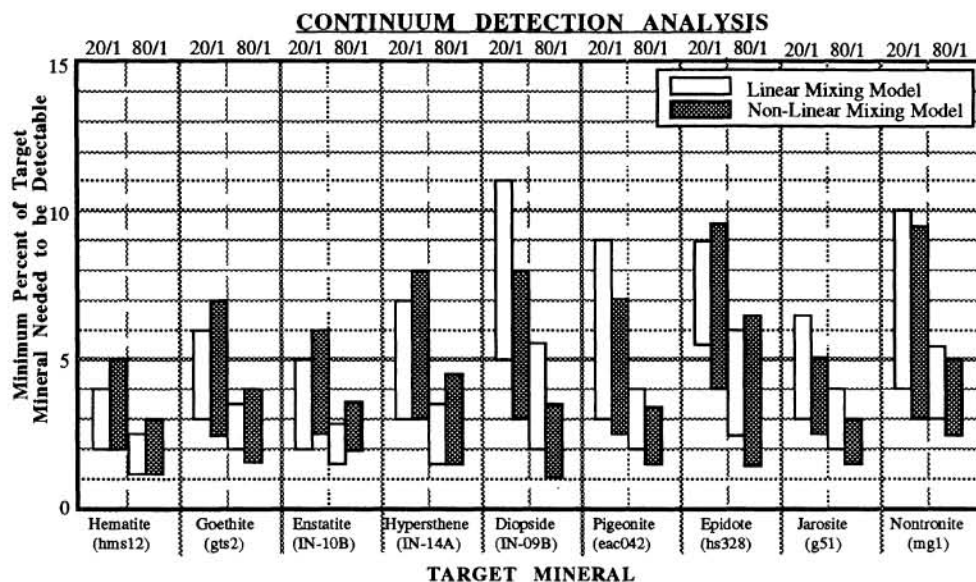


Figure 1: Continuum detection thresholds for a suite of iron-bearing minerals in a background composed of Basalt (LS-CMP-001) and Palagonite (PN9\_20). The range of detection thresholds for each mineral varies with the fractions of the background. The results for both linear and non-linear models are shown at both 20/1 and 80/1 signal-to-noise ratios.

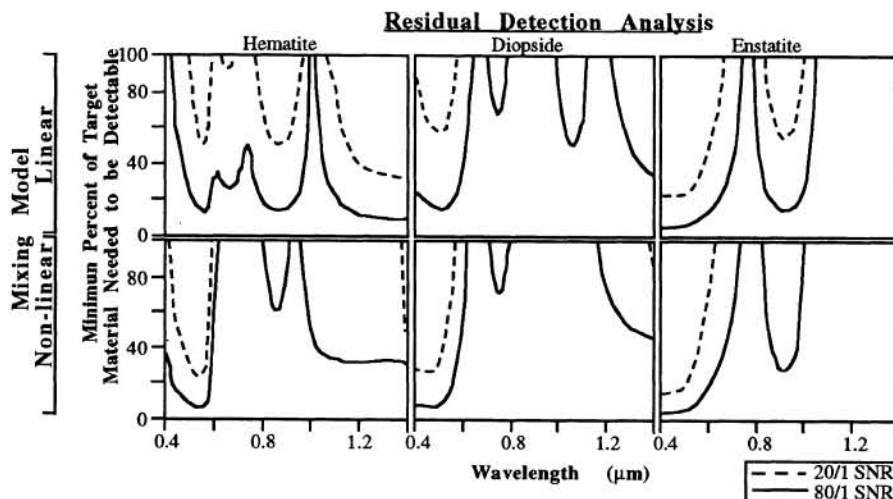


Figure 2: Residual detection thresholds for hematite, diopside, and enstatite in the same background as in figure 1.

**References:** [1] Bell J.F. III et al. (1991) LPI-MSATT Tech Report 92-04, 2. [2] Bell J.F. III et al. (1992) LPSC XXIII, 81. [3] Bell J.F. III et al. (1990) JGR, 95, 14447. [4] Singer R.B. et al. (1979) JGR, 84, 8415. [5] Morris R.V. et al. (1989) JGR, 94, 2760. [6] Bell J.F. III et al. (1993) JGR, in press. [7] Toulmin P. et al. (1977) JGR, 82, 4625. [8] Pollack J.B. et al. (1977) JGR, 82, 4479. [9] Burns R.G. (1987) JGR, 92, E570. [10] Sabol D.E. Jr. et al (1992) JGR, 97, 2659.